Supplementary Information

Writing DNA Bases into sp^3 Quantum Defects

Abhindev Kizhakke Veetil,[1] Alexander Kotsanos,[1] Anna Y. Wang,[2] Fatemeh Hajikarimi,[1] Jacob Fortner,[3] Zhulfaa Zhulficar,[1] Ebenezer Afriyie,[1] YuHuang Wang[1,3,4]*

1 Department of Chemistry and Biochemistry, University of Maryland, College Park, MD 20742, United States
2 Atholton High School, 6520 Freetown Rd, Columbia, MD 21044, United States
3 Chemical Physics Program, University of Maryland, College Park, MD 20742, United States
4 Maryland NanoCenter, University of Maryland, College Park, MD 20742, United States
*Correspondence should be addressed to Y.H.W. at yhw@umd.edu

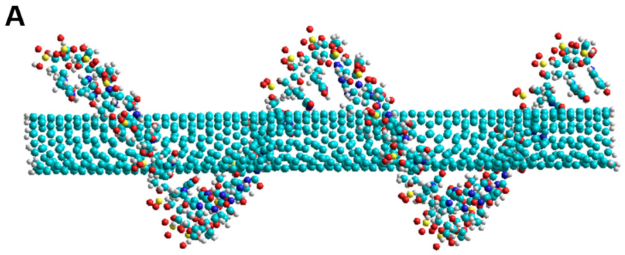

(6,5)-SWCNT@5’-T$_{14}$AT$_{15}$-3’
(5’-T$_{14}$AT$_{15}$-3’ wrapped (6,5)-SWCNT)

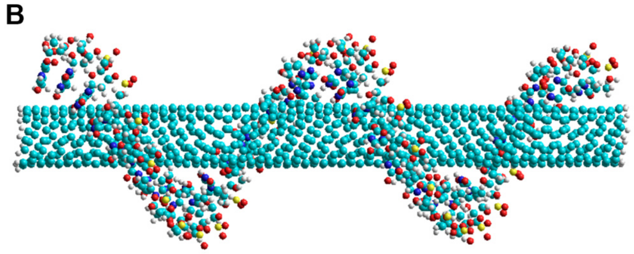

(6,5)-SWCNT—5’-T$_{14}$AT$_{15}$-3’
(5’-T$_{14}$AT$_{15}$-3’ covalently bonded to (6,5)-SWCNT at adenine)

Figure S1. Molecular models of a (6,5)-SWCNT@5′-T$_{14}$AT$_{15}$-3′ (5′-T$_{14}$AT$_{15}$-3′ DNA-wrapped (6,5)-SWCNT) before (A) and after (B) OCC formation, which creates (6,5)-SWCNT—5′-T$_{14}$AT$_{15}$-3′ (5′-T$_{14}$AT$_{15}$-3′ covalently bonded to (6,5)-SWCNT at the adenine site through a carbon-adenine bond). The helical periodicity of the DNA wrapping is largely preserved upon covalent modification.

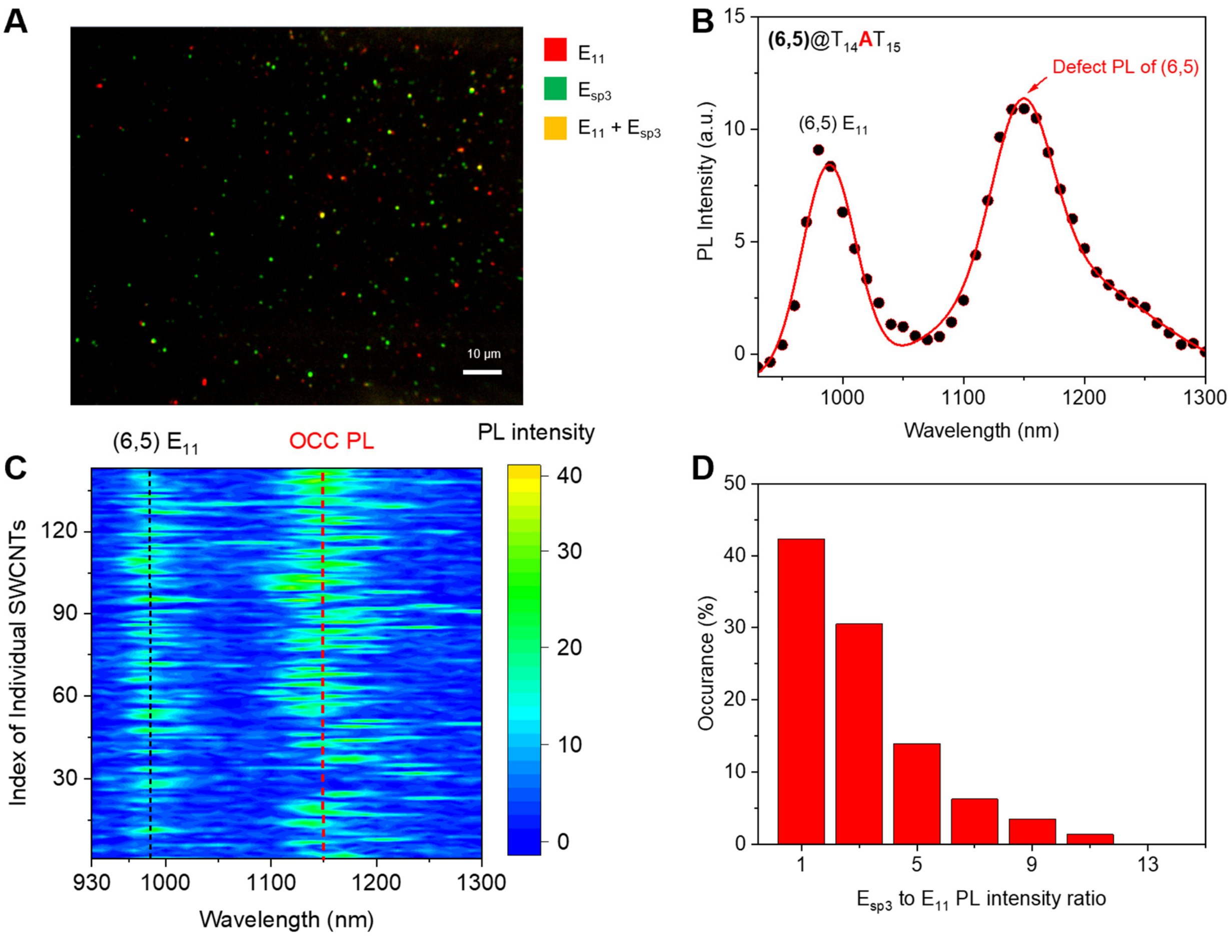

Figure S2. Light triggers OCC formation in (6,5)-SWCNT@DNA. 5′-$\mathrm{T_{14}AT_{15}}$-3′-wrapped (6,5)-SWCNTs form OCCs upon irradiation with 561 nm laser at 54 W/ $\mathrm{cm^2}$ for five minutes. (A) False-color images of (6,5)-SWCNTs functionalized with adenine DNA ($\mathrm{T_{14}AT_{15}}$ E_{11} emission (930 - 1030 nm) is shown in red and E_{sp3} emission (1100 -1300 nm) in green. The orange color shows emitters that contain both E_{11} and E_{sp3}. The green and yellow color spots in the image represent (6,5)-SWCNTs with OCCs. (B) Averaged photoluminescence spectra of (6,5)-SWCNTs samples, showing the emergence of an OCC peak at 1148 nm following adenine OCC formation. (C) Emission spectra of individual SWCNTs irradiated with light. (D) Histograms of E_{sp3}/E_{11} intensity ratios for individual nanotubes.

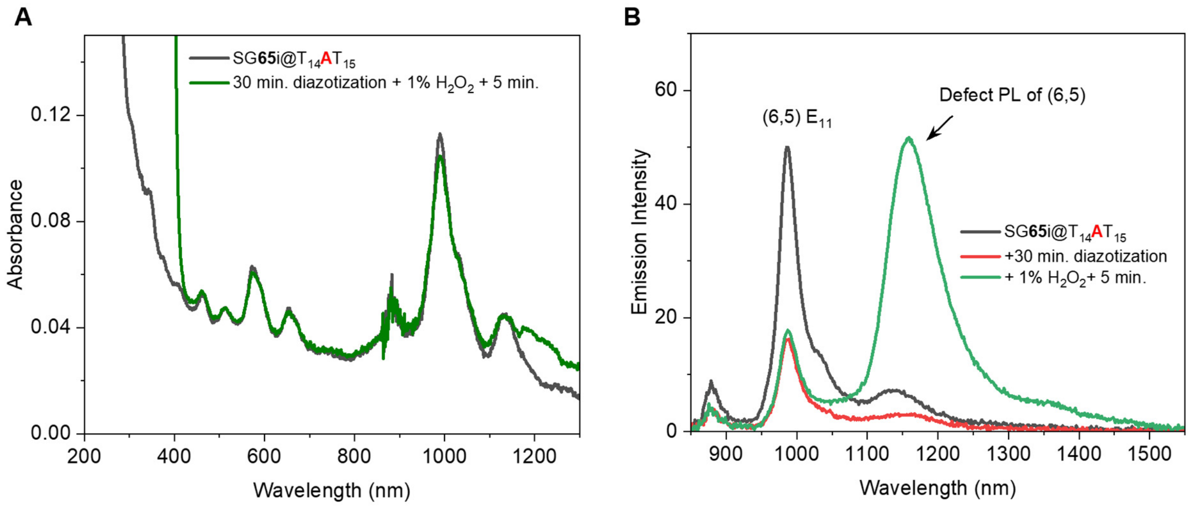

Figure S3. H_2O_2 triggers and accelerates OCC formation within SWCNT@DNA complexes. (A) Absorption spectra of 5′-$T_{14}AT_{15}$-3′-wrapped SG65i nanotubes before reaction (black trace) and after diazotization followed by 1% H_2O_2 trigger (green trace). (B) Photoluminescence spectra (excited at 565 nm) of pristine (black), diazotized (red), and H_2O_2-triggered (green) samples. H_2O_2 induces rapid OCC formation within 5 minutes. The H_2O_2-triggered reaction pathway is generalizable to cytosine and guanine systems.

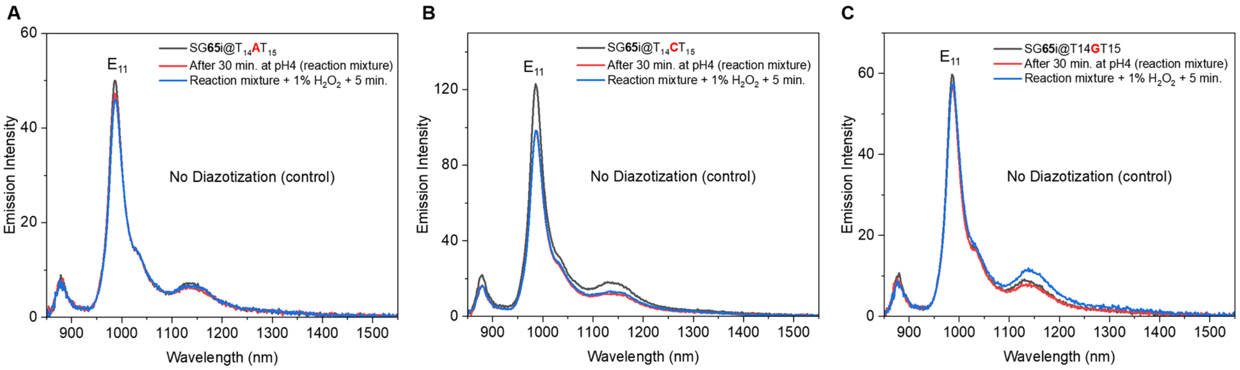

Figure S4. Diazotization is required for OCC formation; H_2O_2 alone does not induce covalent bonding. Photoluminescence spectra of SG65i SWCNTs wrapped with (A) 5′-$T_{14}AT_{15}$-3′, (B) 5′-$T_{14}CT_{15}$-3′, and (C) 5′-$T_{14}GT_{15}$-3′ sequences under three conditions: pristine (black), acid-treated (pH 4) without sodium nitrite (red), and acid + 1% H_2O_2 (blue). The spectra were collected at an excitation wavelength of 565 nm. No OCCs appear without diazotization.

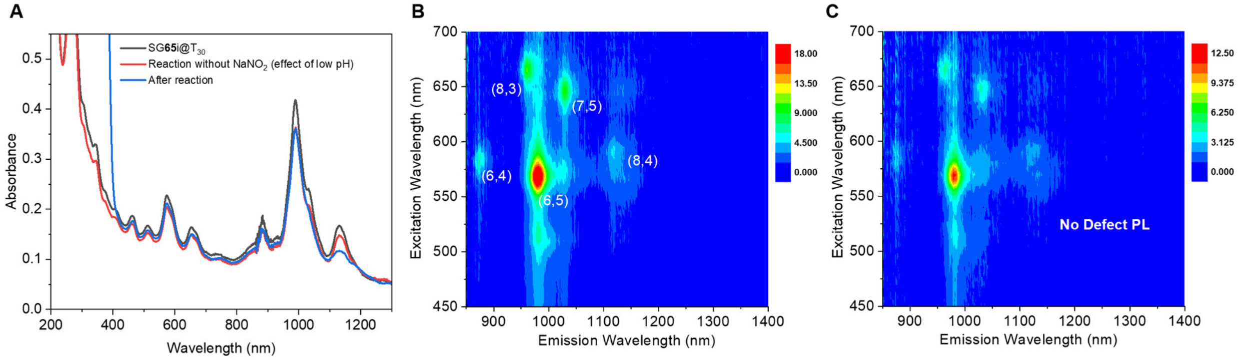

Figure S5. Thymine does not form OCCs because it lacks the primary amines required for diazotization. (A) Absorption spectra of 5′-T_{30}-3′-wrapped SG65i nanotubes before (black trace) and after (blue trace) reaction with the diazotization agent $NaNO_2$. The $NaNO_2$ absent control shows similar spectral changes, indicating that the minor changes arise from acidic conditions rather than covalent functionalization. (B) Photoluminescence excitation-emission map of the pristine sample showing the presence of multiple SWCNT chiralities, including but not limited to (6,5). (C) Photoluminescence excitation-emission map after reaction shows no emergence of the characteristic OCC defect peak near 1150 nm, confirming that thymine does not support diazonium-based covalent modification.

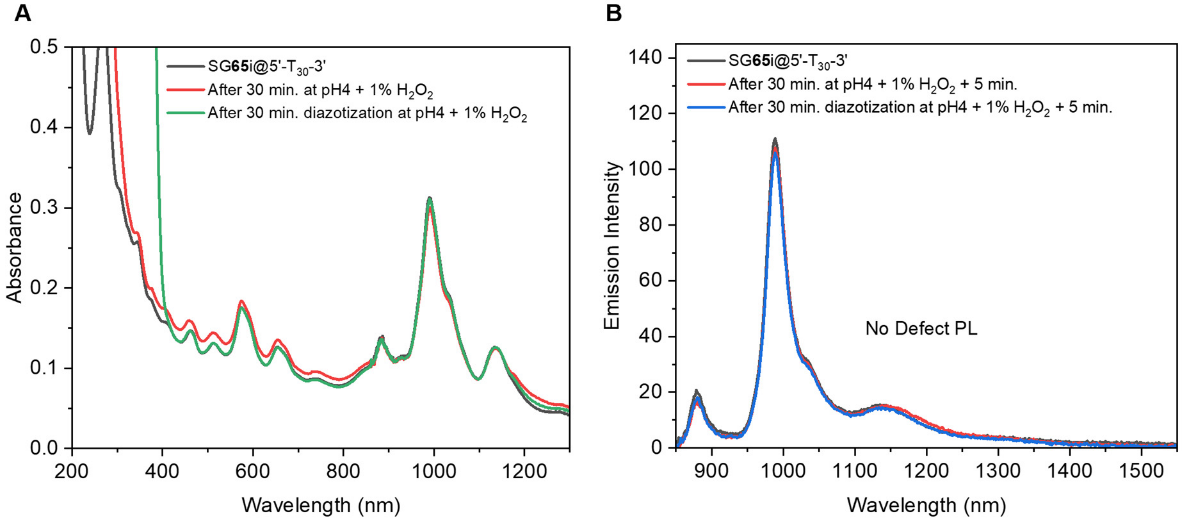

Figure S6. Thymine does not form OCCs even under H_2O_2 triggering. (A) Absorption spectra of 5′-T_{30}-3′-wrapped SG65i SWCNTs before (black trace) and after diazotization, followed by treatment with 1% H_2O_2 (green trace). The red trace corresponds to a control sample kept at pH 4 and treated with 1% H_2O_2without diazotization. Minimal changes in absorption indicate that no covalent reaction occurred. (B) Photoluminescence spectra of the pristine sample (black trace) are nearly identical to those of the diazotized and acid-treated samples exposed to H_2O_2. The characteristic OCC emission near 1150 nm is absent, confirming that thymine does not participate in OCC formation, even under H_2O_2triggering.

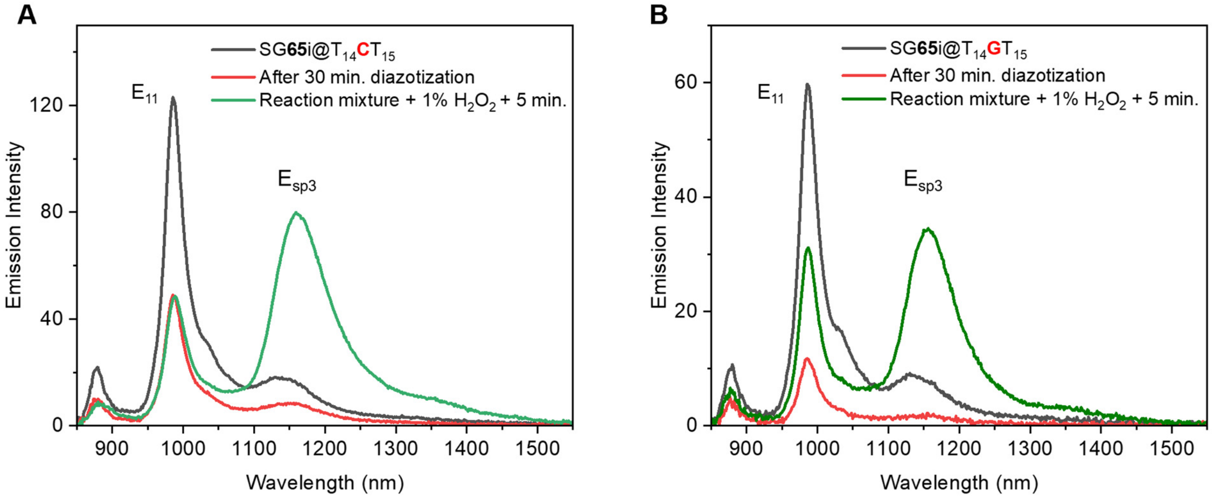

Figure S7. OCC formation extends to cytosine and guanine. (A) Photoluminescence spectra of 5'-$T_{14}CT_{15}$-3' wrapped SG65i before reaction (black), after diazotization (red), and after H_2O_2-triggered OCC formation (green). The spectra were collected at an excitation wavelength of 565 nm. (B) Photoluminescence spectra of 5'-$T_{14}GT_{15}$-3' wrapped SG65i before reaction (black), after diazotization (red), and H_2O_2-triggered OCC formation (green).

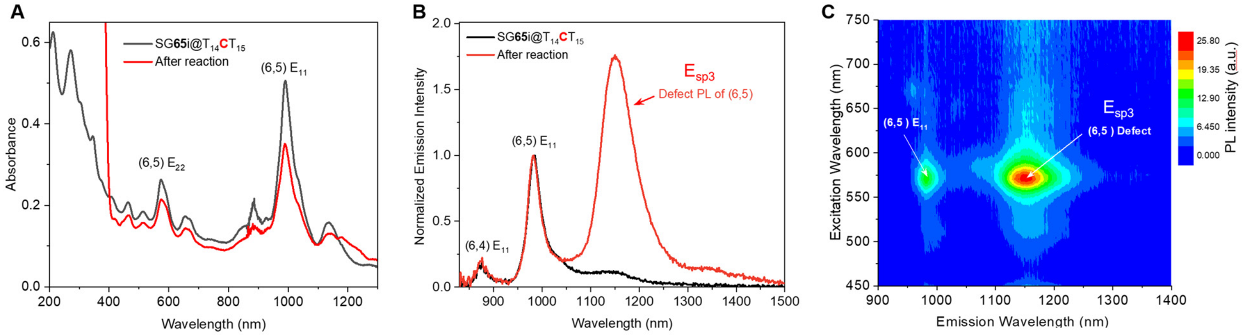

Figure S8. OCC formation via cytosine diazotization in DNA-wrapped (6,5)-SWCNTs. (A) Absorption spectra of 5′-$T_{14}CT_{15}$-3′-wrapped SG65i SWCNTs before (black trace) and after (red trace) diazonium reaction. (B) Photoluminescence spectra showing the emergence of a defect peak at 1150 nm under E_{22} excitation. (C) Excitation-emission map of the functionalized sample confirms that the defect emission arises from the (6,5)-SWCNT.

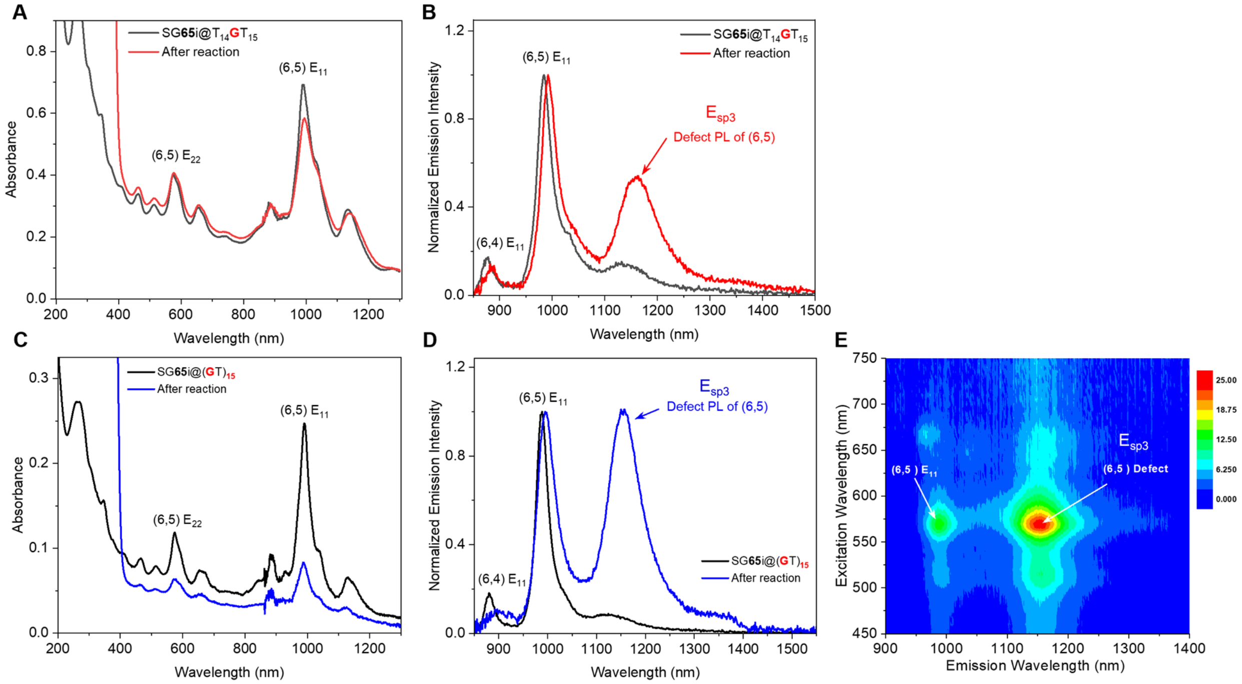

Figure S9. OCC formation via guanine diazotization in DNA-wrapped (6,5)-SWCNTs. (A) Absorption spectra of 5′-T$_{14}$GT$_{15}$-3′-wrapped SG65i SWCNTs before (black trace) and after (red trace) the DNA diazonium reaction. (B) Photoluminescence spectra of pristine (black trace) and functionalized (red trace) samples excited at 565 nm, revealing a defect emission at 1162 nm indicative of guanine-OCC formation. (C) Absorption spectra of 5′-(GT)$_{15}$-3′-wrapped SG65i SWCNTs before (black trace) and after (blue trace) the DNA diazonium reaction. (D) Photoluminescence spectra of pristine (black trace) and functionalized (blue trace) samples excited at 565 nm, showing a red-shifted defect peak at 1155 nm, attributed to OCC formation at multiple guanine sites. (E) Photoluminescence excitation-emission map of the functionalized (GT)$_{15}$ sample confirms the emission arises from modified (6,5)-SWCNTs.

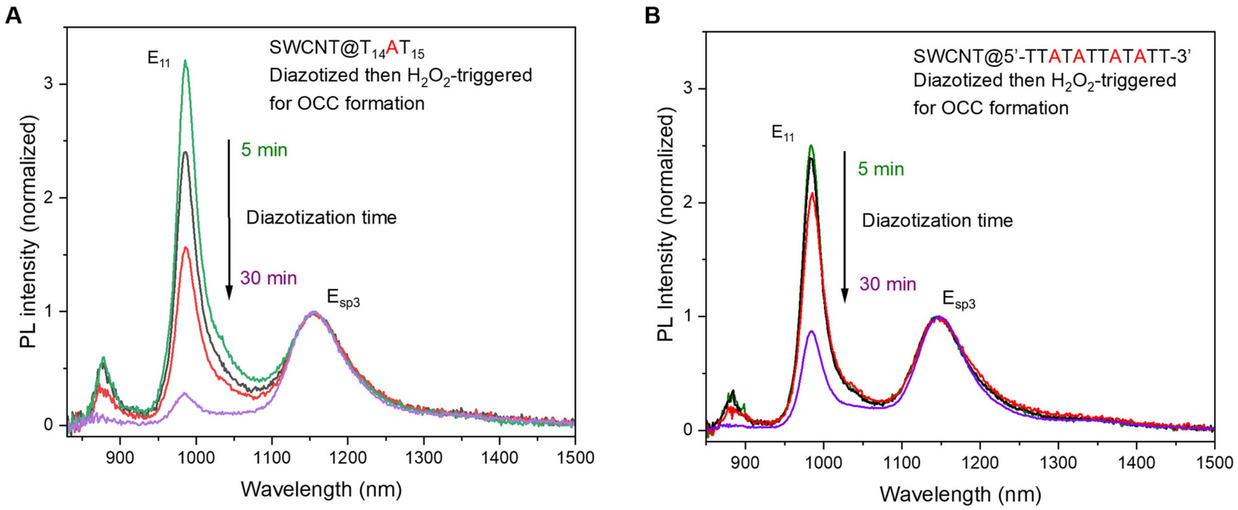

Figure S10. OCC emission energy is independent of the degree of functionalization. (A) PL spectra of 5′-T$_{14}$**A**T$_{15}$-3′-wrapped SG65i SWCNTs with different degrees of functionalization. (B) PL spectra of 5′-TT**A**T**A**TT**A**T**A**TT-3′ wrapped SG65i SWCNTs with a different degree of functionalization. In all cases, the excitation line is 565 nm. The OCC peak positions remain unchanged regardless of the degree of functionalization achieved by varying the diazotization time. This observation supports the notion that the 10 meV shift we observe between cytosine and guanine OCCs arises from their chemical differences, rather than from defect density. The OCC formation reaction was triggered with 1% H_2O_2, and varying diazotization times resulted in varying degrees of functionalization, as shown in the images: 5 minutes (green), 10 minutes (black), 15 minutes (red), and 30 minutes (violet).

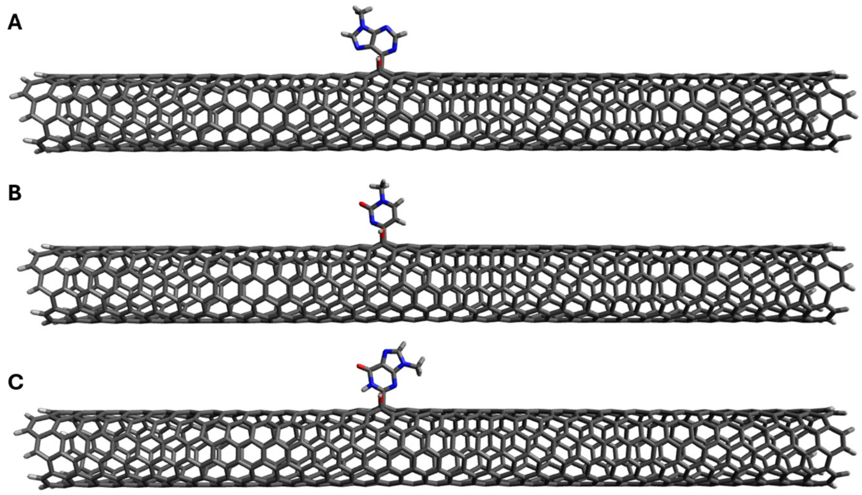

Figure S11. Geometry optimized molecular models used for TD-DFT calculations. OCCs are made from A) adenine, B) cytosine, or C) guanine with the $–NH_2$ group replaced by the bond to the SWCNT surface and an –OH group bound in the ortho-90 binding configuration.

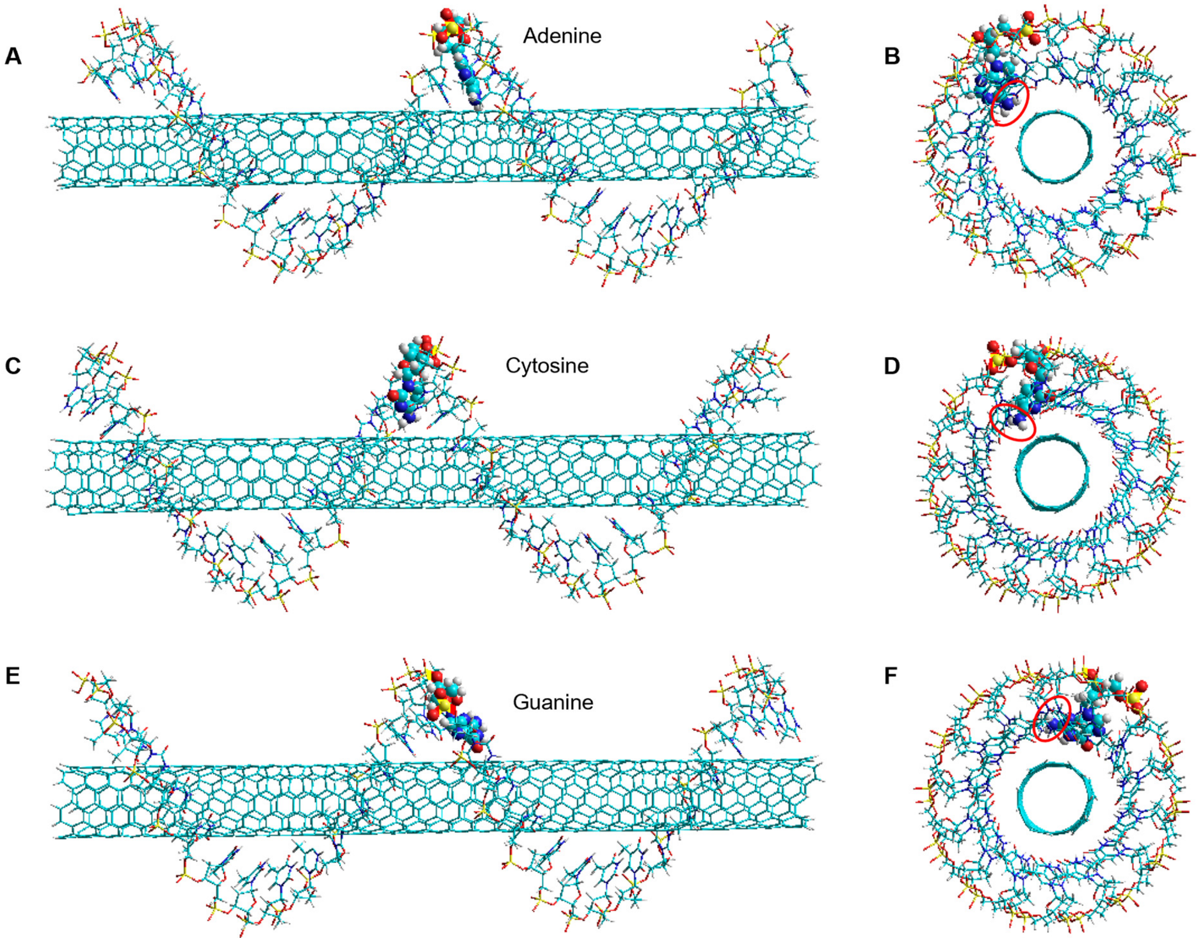

Figure S12. Structural models of DNA orientation on pristine SWCNTs. Side and front views of (6,5)-SWCNTs wrapped with (A, B) 5′-$T_{14}AT_{15}$-3′, (C, D) 5′-$T_{14}CT_{15}$-3′, and (E, F) 5′-$T_{14}GT_{15}$-3′, respectively. The primary aromatic amine groups (highlighted in red circles) exhibit basedependent orientations that influence the accessibility and reactivity of the diazotized nucleobases toward the SWCNT.

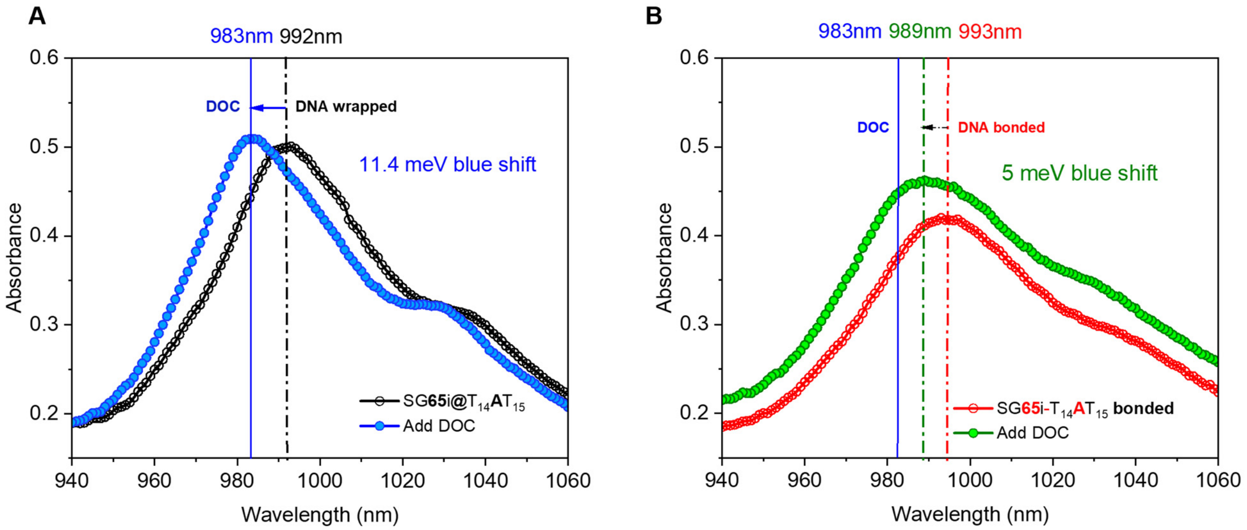

Figure S13. DNA-to-DOC exchange experiments confirm the stability of covalently bound DNA. (A) For pristine DNA-wrapped SWCNTs, the addition of 1% DOC blueshifts the E_{11} absorption peak to 983 nm, indicating the complete displacement of the non-covalently bound DNA by DOC. (B) For covalently bonded DNA, DOC induces only a partial shift (to 989 nm), showing that covalently attached DNA remains stably bound to the SWCNT.

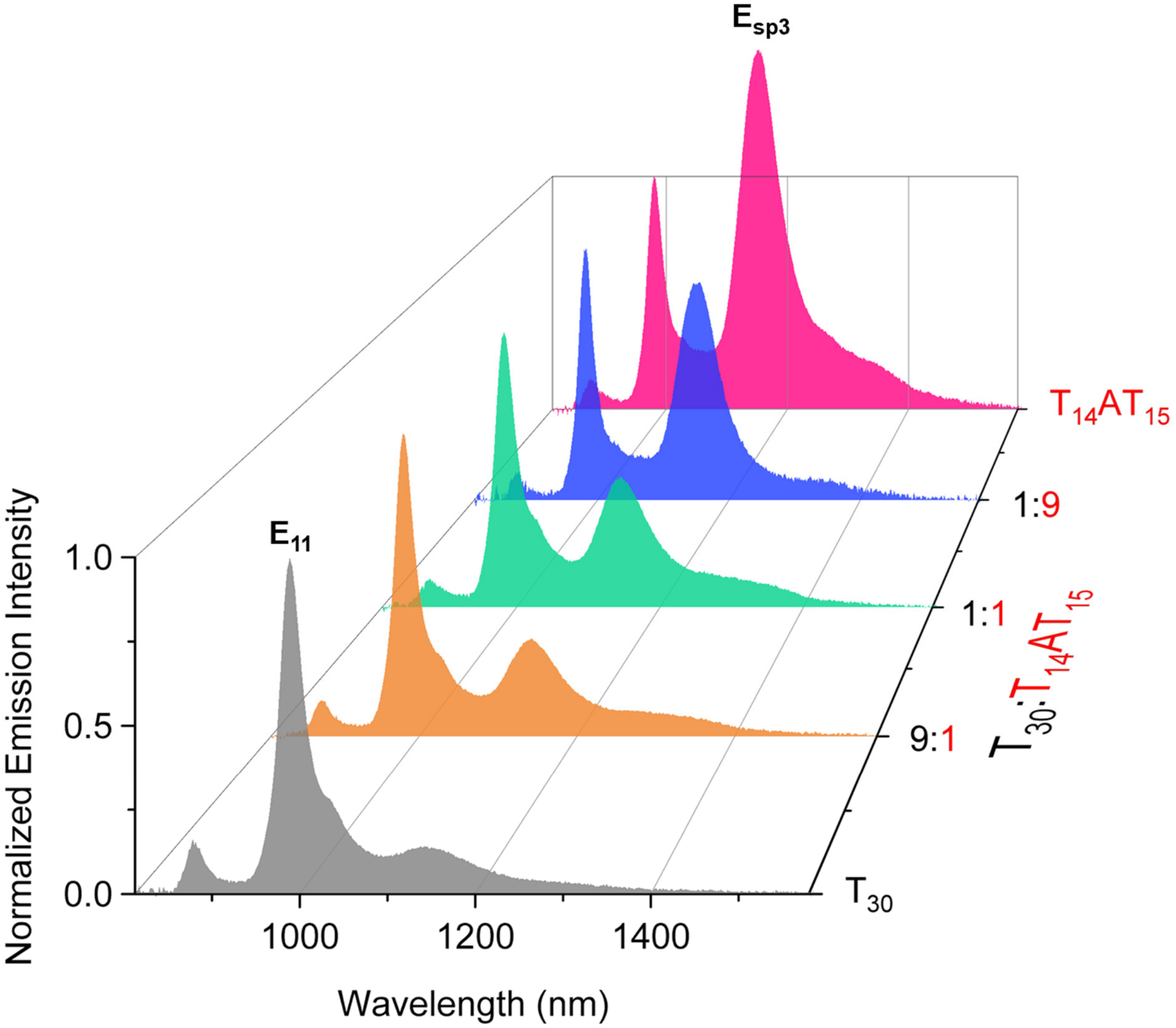

Figure S14. Thymine sequences act as inert spacers controlling OCC density. Photoluminescence spectra of 5′-$T_{14}AT_{15}$-3′-functionalized SG65i SWCNTs with increasing amounts of T_{30} inert sequences. Higher concentrations of T_{30} reduce OCC formation, indicating effective modulation of defect density.